Journal of Medicinal Chemistry

pubs.acs.org/jmc

Article

Fragment-like Chloroquinolineamines Activate the Orphan Nuclear Receptor Nurr1 and Elucidate Activation Mechanisms

Sabine Willems, Julia Ohrndorf, Whitney Kilu, Jan Heering, and Daniel Merk*

Cite This: J. Med. Chem. 2021, 64, 2659−2668

Read Online

ACCESS | Metrics & More | Article Recommendations | Supporting Information

ABSTRACT: The ligand-activated transcription factor nuclear receptor related-1 (Nurr1) exhibits great potential for neurodegenerative disease treatment, but potent Nurr1 modulators to further probe and validate the nuclear receptor as a therapeutic target are lacking. We have systematically studied the structure−activity relationship of the 4-amino-7-chloroquinoline scaffold contained in Nurr1 activators amodiaquine and chloroquine and discovered fragment-like analogues that activated Nurr1 in several cellular settings. The most active descendants promoted the transcriptional activity of Nurr1 on human response elements as monomer, homodimer, and heterodimer and markedly enhanced Nurr1-dependent gene expression in human astrocytes. As a tool to elucidate mechanisms involving in Nurr1 activation, these Nurr1 agonists induced robust recruitment of NCoR1 and NCoR2 co-regulators to the Nurr1 ligand binding domain and promoted Nurr1 dimerization. These findings provide important insights in Nurr1 regulation. The fragment-sized Nurr1 agonists are appealing starting points for medicinal chemistry and valuable early Nurr1 agonist tools for pharmacology and chemical biology.

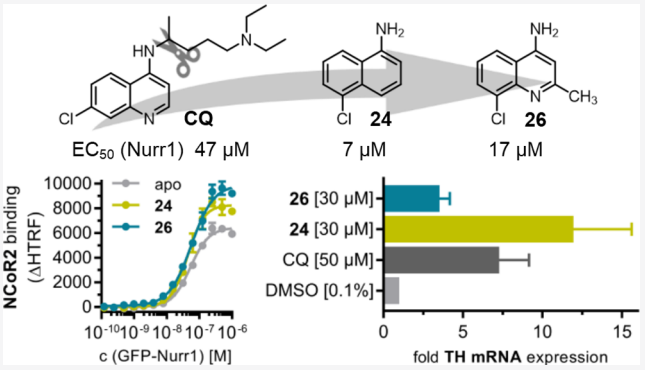

INTRODUCTION

The ligand-sensing transcription factor nuclear receptor related-1 (Nurr1, NR4A2)[1] is an orphan nuclear receptor with neuroprotective properties. Nurr1 is found in several neuronal cells with particularly high expression in dopaminergic neurons.[2] It regulates the expression of various genes in dopamine metabolism and transport, which turned out to be crucial for the protection and survival of dopaminergic neurons.[2] Altered expression of Nurr1 in patients of Parkinson's Disease (PD) and the observation that neuronal Nurr1 knockout in mice causes a phenotype resembling PD further point to high therapeutic potential of Nurr1 modulation in PD and other neurodegenerative pathologies.[2,3] The prostaglandins PGA1 and PGE1 were recently discovered as endogenous Nurr1 ligands with intermediate micromolar potency and neuroprotective effects.[4] However, the lack of potent Nurr1 modulators as tools hinders further evaluation and validation of Nurr1 as a therapeutic target.

Amodiaquine (AQ, **1**), chloroquine (CQ, **2**), and glafenine (**3**) have been reported as first-in-class activators of Nurr1[3] with micromolar activity (Table 1). These compounds importantly demonstrate that Nurr1 can be activated with small molecules. However, their limited potency and their effects on various other proteins and signaling pathways[5−13] render them insufficient as tools for pharmacology and chemical biology. Optimized Nurr1 activators are required to study the role of the orphan nuclear receptor in health and disease.

Munoz-Tello et al.[13] have recently demonstrated that among the putative Nurr1 modulators reported in the literature, only AQ (**1**), CQ (**2**), and cytosporone B act as direct ligands of the nuclear receptor to control its transcriptional activity. Moreover, this recent study confirms previous observations that AQ (**1**) and CQ (**2**) likely target the canonical ligand binding site of the Nurr1 ligand binding domain (LBD)[3] in contrast to PGA1 and PGE1, which bind to a noncanonical site between helices H5, H11, and H12.[4] These important findings[13] make the AQ/CQ chemotype of Nurr1 modulators an attractive starting point for the development of Nurr1 targeting tool compounds.

Using **1**−**3** as the starting matter, we have assessed the structure−activity relationship (SAR) of this AQ chemotype of Nurr1 ligands by a rapid fragment-based strategy. We have discovered that the 4-amino-7-chloroquinoline (**4**) scaffold alone is sufficient for Nurr1 activation despite low potency. By

Received: October 19, 2020
Published: February 25, 2021

Table 1. SAR of Side-Chain Motifs in the AQ/CQ Chemotype. Biological Activity of 1−10 on Nurr1 In Vitro[a]

ID	R	Nurr1 Activity type	Nurr1 EC_{50} (max. fold act.)
1 (AQ)	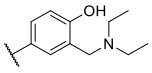	Agonist	36±4 μM (3.6±0.1)
2 (CQ)	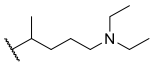	Agonist	47±5 μM (2.0±0.1)
3	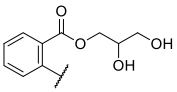	inactive (10 μM)[b]	
4	-H	Agonist	259±70 μM (2.5±0.4)
5	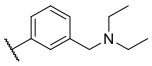	Agonist	116±4 μM (3.1±0.2)
6	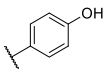	inactive (30 μM)[b]	
7	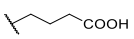	Inverse agonist	IC_{50}=132±1 μM
8		Agonist	1.8±0.3 μM (1.47±0.03)
9		inactive (30 μM)[b]	
10		inactive (10 μM)[b]	

[a]Activity was determined in a Gal4-Nurr1 hybrid reporter gene assay. EC_{50} and IC_{50} values are the mean ± SD; $n \geq 3$. Max. fold activation refers to fold reporter activity compared to DMSO (0.1%)-treated cells. [b]Inactive: no significant effect on reporter activity (≥1.5-fold activation or compared to Gal4-VP16 at the highest nontoxic concentration as indicated).

systematically varying its substitution pattern, we discovered potent, fragment-like Nurr1 agonists (**24** and **26**), which activated Nurr1 in cellular and cell-free settings. **26** evolves as a valuable chemical tool to probe molecular mechanisms of Nurr1 activation. In contrast to AQ and CQ, whose tool compound applicability is hindered by nonspecific effects on transcriptional activity,[13] **26** overcomes this limitation. Using **26** for functional studies, we observed robust recruitment of the nuclear receptor co-regulators NCoR1 and NCoR2 to Nurr1 by **26** and a promoting effect on Nurr1 homodimerization, which provide improved understanding of molecular Nurr1 activation mechanisms.

RESULTS AND DISCUSSION

Chemistry. Nurr1 modulators **4**−**33** were synthesized according to Schemes 1 and 2 or commercially available. **6** and **29**−**33** were prepared from the respective 4-chloroquinolines **12** and **34** and the respective amines **35**−**40** by nucleophilic aromatic substitution according to a previously reported procedure to **6**[14] with suitable adaptions (Scheme 1). **27** and **28** were generated by reductive amination from 5-chloronapthalen-1-amine (**24**) and the respective ketones **41** and **42** (Scheme 2).

Scheme 1. Synthesis of 6 and 29−33[a]

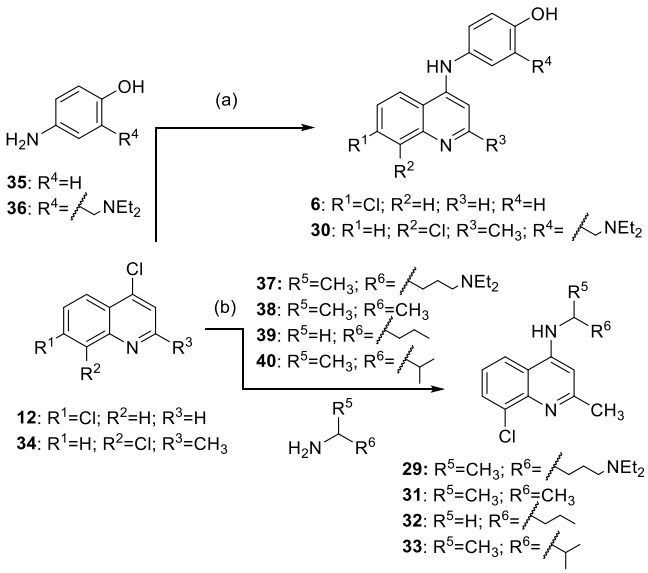

[a]Reagents and conditions: (a) KI, EtOH, 2 N HCl, 90 °C, 14−20 h; (b) EtOH, *μw*, 140 °C, 36−48 h.

Scheme 2. Synthesis of 27 and 28[a]

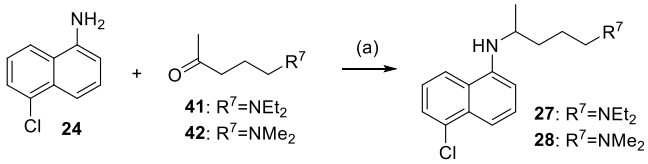

[a]Reagents and conditions: (a) HOAc, DCE, room temperature, 30 min; then $NaB(OAc)_3H$, DCE, 50 °C, 24 h.

Biological Evaluation. A cellular hybrid reporter gene assay in HEK293 cells served as a primary test system to determine Nurr1 modulation by **1**−**33**. This assay is based on a hybrid receptor construct composed of the human Nurr1 LBD and the Gal4 DNA binding domain from yeast. A Gal4-sensitive firefly luciferase construct served as the reporter gene, and constitutively expressed renilla luciferase (SV40 promoter) was used to normalize for transfection efficiency and to monitor test compound toxicity. In agreement with the constitutively active nature of Nurr1,[1] the chimeric Gal4-Nurr1 receptor displays strong intrinsic transcriptional inducer activity also in the absence of a ligand. As a control experiment, all tested compounds were assessed for unspecific effects on reporter activity in an analogous setting with the potent transcriptional inducer Gal4-VP16[15] replacing Gal4-Nurr1 (Figure S1). By providing insights into the type of activity (agonist or inverse agonist), potency, and efficacy of the tested compounds, this hybrid reporter gene assay appeared as the most suitable primary test system, especially since knowledge on Nurr1-interacting co-regulators and their response to ligands as the basis for cell-free recruitment assays is still limited.[16]

For further insights into cellular Nurr1 modulation in more physiological settings, selected compounds were profiled for activation of full-length human Nurr1 as the monomer, homodimer, or RXR-heterodimer. For this, firefly reporter

https://dx.doi.org/10.1021/acs.jmedchem.0c01779
J. Med. Chem. 2021, 64, 2659−2668

constructs comprising a single repeat of the respective human response elements of monomeric Nurr1 (NBRE), the Nurr1 homodimer (NurRE), or the RXR-Nurr1 heterodimer (DR5) in front of the reporter gene were used. Nurr1 and, in the case of DR5, also RXRα were overexpressed using CMV promoter-dependent expression constructs. As for the hybrid Gal4-Nurr1 assay, constitutively expressed renilla luciferase served for normalization purposes. In addition, effects of selected compounds on Nurr1-regulated gene expression were evaluated in Nurr1 expressing[17] T98G glioblastoma cells on the mRNA level by quantitative real-time polymerase chain reaction (qRT-PCR).

Nurr1 modulation was also studied in cell-free, homogeneous time-resolved fluorescence resonance energy transfer (HTRF)-based settings using Tb^{3+}-cryptate-labeled co-regulator peptides derived from NCoR1 and NCoR2 as FRET donors and recombinant, GFP-labeled Nurr1 LBD protein as the FRET acceptor.

Structure–Activity Relationship. All three reported Nurr1 activators AQ (**1**), CQ (**2**), and glafenine (**3**) share an identical 4-amino-7-chloroquinoline scaffold prompting the hypothesis that this shared structural feature strongly contributes to their biological activity on Nurr1. To preliminarily test this assumption, we determined the Nurr1 modulatory activity of a small series of further 4-amino-7-chloroquinoline derivatives (**4**–**10**, Table 1).

AQ (**1**) and CQ (**2**) activated Gal4-Nurr1 with intermediate micromolar EC_{50} values of 36 ± 4 μM (3.6 ± 0.1 max. fold activation) and 47 ± 5 μM (2.0 ± 0.1 max. fold activation), respectively, which agreed with their reported activities[3] and validated our in vitro test system. Glafenine (**3**) turned out to be too toxic to be reasonably characterized in the cellular setting. The minimal shared structure 4-amino-7-chloroquinoline (**4**) of AQ (**1**) and CQ (**2**) was indeed sufficient to activate Nurr1 despite lower potency in a high micromolar range. AQ analogue **5** lacking the phenolic hydroxyl group retained reduced Nurr1 agonistic potency, too, while removal of the diethylaminomethyl motif (**6**) resulted in full loss of activity. Replacement of the basic side chain of AQ (**1**) and CQ (**2**) by a butyric acid motif of similar size in **7** produced an inverse agonist that markedly reduced the transcriptional activity of Nurr1. A small lipophilic isopentyl side chain residue (**8**) recovered Nurr1 agonism with a remarkable 1.8 μM EC_{50} value but low activation efficacy. The bulkier 4-methylcyclohexyl- (**9**) and benzyl- (**10**) derivatives failed to modulate Nurr1 activity. These preliminary SAR observations indicate that the side chain motif contributes to Nurr1 modulation but characterize the 4-amino-7-chloroquinoline (**4**) as the key structural feature for Nurr1 modulation. Intrigued by the observation that the fragment-sized structure **4** was sufficient to activate Nurr1, we studied the SAR of the isolated chloroquinoline-amine motif individually.

First, we evaluated the individual contributions of structural features of **4** to Nurr1 activation by their systematic removal (Table 2). 7-Chloroquinoline (**11**) lacking the 4-amino group revealed inverse Nurr1 agonism with moderate repressor efficacy, while 4,7-dichloroquinoline (**12**) was inactive pointing to an important contribution of the amino group to Nurr1 activation. 4-Aminoquinoline (**13**) lacking the 7-chlorine substituent was inactive, too, indicating the chlorine as another important feature for Nurr1 agonism. Introduction of an additional methyl group in the 2-position of the 4-amino-7-chloroquinoline (**14**) was accompanied with a remarkable gain in potency by almost a factor of 10 compared to **4**.

Table 2. Contribution of Chlorine and Amine Residues in the Chloroquinolineamine Scaffold. Biological Activity of 11–14 on Nurr1 In Vitro[a]

		Nurr1	
ID	structure	Activity type	EC_{50} (max. fold act.)
4	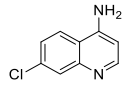	Agonist	259±70 μM (2.5±0.4)
11	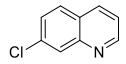	Inverse agonist	IC_{50}=89±14 μM
12	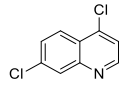	inactive (300 μM)[b]	
13		inactive (300 μM)[b]	
14	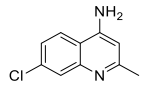	Agonist	33±5 μM (2.3±0.2)

[a]Activity was determined in a Gal4-Nurr1 hybrid reporter gene assay. EC_{50} and IC_{50} values are the mean ± SD; n ≥ 3. Max. fold activation refers to fold reporter activity compared to DMSO (0.1%)-treated cells. [b]Inactive: no significant effect on reporter activity (≥1.5-fold activation or compared to Gal4-VP16 at the highest nontoxic concentration as indicated).

We then systematically varied the regiochemistry of the essential chlorine and amine substituents (Table 3). Shifting the chlorine atom from the 7- (**4**) to the 6- (**15**) or 8-position (**16**) strongly promoted potency on Nurr1, with 8-chloro-4-aminoquinoline (**16**) as the most favored isomer. For the amine substituent, agonism on Nurr1 was lost when the amino group was moved from the 4-position in **4** to the 2- (**17**) or 3-position (**18**), while shifting the amine to the benzoid ring in the 5-position (**19**) was favored by Nurr1. However, this structural modification turned out to be incompatible with the favored 6- (**15**) or 8-position (**16**) of the chlorine substituent since 6-chloro-5-aminoquinoline (**20**) and 8-chloro-5-aminoquinoline (**21**) were inactive. When we replaced the 8-chlorine substituent of the preferred chloroquinolineamine isomer **16** by a bulkier trifluoromethyl group (**22**) or by a smaller fluorine atom (**23**), we observed a drastic loss in potency, suggesting that the chlorine atom was highly favored in this position. Eventually, we also addressed the contribution of the quinoline nitrogen atom in the favored regioisomer **16** whose removal in naphthalene **24** was favored and promoted potency by a factor of 5, whereas shifting the nitrogen by one position to isoquinoline **25** resulted in inactivity.

The in vitro activities of **11**–**25** demonstrated the presence and regiochemistry of the amine and chlorine substituents as crucial contributing factors for potency on Nurr1. Additionally, we observed an increase in potency for a methyl group in the 2-position. Combination of this favorable methyl substituent (**14**) with a preferred regiochemistry of the chlorine and amine substituents (**16**) in **26** further enhanced potency to a low micromolar EC_{50} value (Table 4).

https://dx.doi.org/10.1021/acs.jmedchem.0c01779
J. Med. Chem. 2021, 64, 2659–2668

Table 3. SAR and Biological Activity of Chloroquinoline-Amine Regioisomers 15−25 on Nurr1 In Vitro[a]

ID	structure	Nurr1 Activity type	Nurr1 EC_{50} (max. fold act.)
4	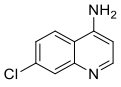	Agonist	259±70 μM (2.5±0.4)
15	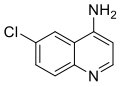	Agonist	117±24 μM (2.8±0.3)
16	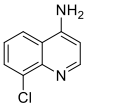	Agonist	49±5 μM (2.6±0.1)
17	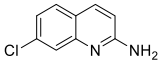	inactive (100 μM)[b]	
18	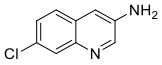	inactive (300 μM)[b]	
19	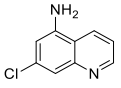	Agonist	19±4 μM (3.4±0.3)
20	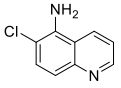	inactive (100 μM)[b]	
21	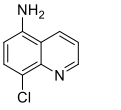	inactive (100 μM)[b]	
22	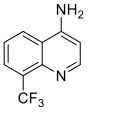	inactive (300 μM)[b]	
23	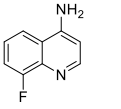	inactive (300 μM)[b]	
24	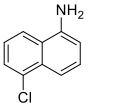	Agonist	7.3±0.5 μM (5.3±0.2)
25	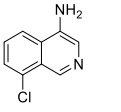	inactive (200 μM)[b]	

[a]Activity was determined in a Gal4-Nurr1 hybrid reporter gene assay. EC_{50} values are the mean ± SD; n ≥ 3. Max. fold activation refers to fold reporter activity compared to DMSO (0.1%)-treated cells. [b]Inactive: no significant effect on reporter activity (≥1.5-fold activation or compared to Gal4-VP16 at the highest nontoxic concentration as indicated).

Our systematic SAR analysis of **4** and analogues as Nurr1 agonists rendered **24** and **26** as the most favorable derivatives. With EC_{50} values of 7 and 17 μM, respectively, both fragment-like molecules **24** and **26** possess slightly higher potencies on Nurr1 than the template drugs AQ (**1**) and CQ (**2**) while

Table 4. Fused SAR in the Chloroquinolineamine Fragment. Biological Activity of 14, 16, and 26 on Nurr1 In Vitro[a]

ID	structure	Nurr1 Activity type	Nurr1 EC_{50} (max. fold act.)
14	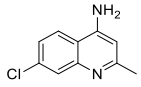	Agonist	33±5 μM (2.3±0.2)
16	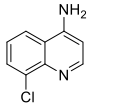	Agonist	49±5 μM (2.6±0.1)
26	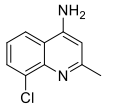	Agonist	17±6 μM (1.71±0.11)

[a]Activity was determined in a Gal4-Nurr1 hybrid reporter gene assay. EC_{50} values are the mean ± SD; n ≥ 3. Max. fold activation refers to fold reporter activity compared to DMSO (0.1%)-treated cells.

comprising markedly lower molecular weights. Accordingly, **24** and **26** are superior in terms of ligand efficiency (LE), lipophilic ligand efficiency (LLE), and size-independent ligand efficiency (SILE)[18] compared to AQ (**1**) and CQ (**2**), which were employed as leads (Table 5).

Table 5. Efficiency Metrics of Nurr1 Agonists[a]

ID	EC_{50} (Nurr1)	LE	LLE[b]	SILE
1	36 ± 4 μM	0.24	−0.39	1.7
2	47 ± 5 μM	0.27	−0.95	1.7
24	7.3 ± 0.5 μM	0.59	1.85	2.4
26	17 ± 6 μM	0.50	1.83	2.2

[a]Metrics were calculated as described in ref 18. [b]alogP for LLE calculations was retrieved from the ALOGPS 2.1 resource.[19]

In an attempt to recombine **24** and **26** with the substituents of the template drugs, we prepared and characterized the respective CQ analogues (Table 6). Compound **27** resulting from fusion of CQ (**2**) and fragment **24** was active but too toxic for full dose−response characterization on Gal4-Nurr1. Its potency was inferior to fragment **24** but might be a minor improvement over CQ (**2**). To exclude steric hindrance as a reason for the surprisingly low potency of **27**, we studied its smaller dimethyl analogue **28**, which was inactive up to 10 μM and toxic at higher concentrations. The fusion of **26** and **2** in **29** was nontoxic but inactive on Gal4-Nurr1 up to high 100 μM concentration. Despite the undesirable nonspecific activities of AQ (**1**),[5−10,20,21] we also fused **26** with the AQ side chain, but the resulting compound **30** was inactive, too. These results suggest that recombination of the optimized fragment with the AQ (**1**) or CQ (**2**) side chains was not a constructive strategy to achieve further optimization.

The early SAR analysis had also revealed a branched lipophilic side chain (**8**) as favored for Nurr1 activation. Hence, we additionally probed fusion of this isopentyl motif and related small lipophilic groups with the optimized chloroquinoline fragment **26** (**31**−**33**, Table 6). All three derivatives comprising an isopropyl (**31**), *n*-butyl (**32**), or isopentyl (**33**) substituent activated Nurr1 with micromolar

https://dx.doi.org/10.1021/acs.jmedchem.0c01779
J. Med. Chem. 2021, 64, 2659−2668

Table 6. Biological Activity of Fused Structures 27−33 on Nurr1 In Vitro[a]

ID	structure	Nurr1 Activity type	Nurr1 EC_{50} (max. fold act.)
27	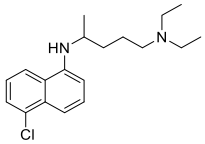	Agonist	EC_{50} n.d., (1.46-fold act. at 20 μM, toxic above)
28	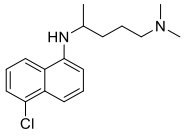	inactive (10 μM)[b], toxic above	
29	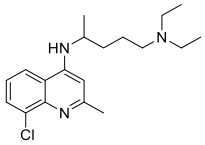	inactive (100 μM)[b]	
30	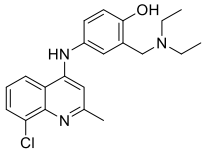	inactive (100 μM)[b]	
31	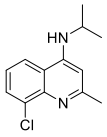	Agonist	31±5 μM (2.0±0.2)
32	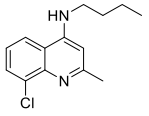	Agonist	12±1 μM (2.4±0.2)
33	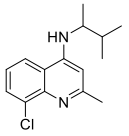	Agonist	17±3 μM (2.3±0.3)

[a]Activity was determined in a Gal4-Nurr1 hybrid reporter gene assay. EC_{50} values are the mean ± SD; n ≥ 3. Max. fold activation refers to fold reporter activity compared to DMSO (0.1%)-treated cells. [b]Inactive: no significant effect on reporter activity (≥1.5-fold activation or compared to Gal4-VP16 at the highest nontoxic concentration as indicated).

potencies, but neither modification provided an improvement in potency compared to the fragment **26**. Together, the weak Nurr1 modulatory activities of the fused derivatives **27**−**33**, hence, indicate that the SAR of the chloroquinoline core and the side chain motif is not additive and that systematic efforts are needed for further optimization.

While compound **24** evolved as the most potent Nurr1 agonist in this study, it also exhibited nonspecific effects on the control gene (renilla luciferase) in our reporter gene assays (Figures S2a and S3). Its efficacy in Nurr1 activation may therefore be overestimated. Control experiments on Gal4-VP16 (Figure S1) and a pronounced increase in Nurr1-induced reporter activity demonstrate, however, that **24** activates Nurr1 despite nonspecific effects. Of note, the previously reported Nurr1 agonists CQ (**2**) and especially AQ (**1**) cause opposite nonspecific effects on control gene activity (Figure S2a), indicating nonspecific transcriptional activation as already observed by Munoz-Tello et al.[13] Compound **26**, in contrast, did not affect renilla activity (Figure S2a) and VP16-dependent transcriptional activity (Figure S1), suggesting it as an improved Nurr1 agonist tool with reduced nonspecific effects.

Based on these considerations, **26** evolved as the most attractive fragment descendant of AQ (**1**) and CQ (**2**) for further studies on Nurr1 agonist characteristics. In addition, fragment **24** presents as an attractive starting point for further optimization despite nonspecific activity that will require attention (Figure S2). Hence, we studied the effects of **24** and **26** on Nurr1 activity in more physiological settings involving the full-length human nuclear receptor (Figure 1a and 1b;

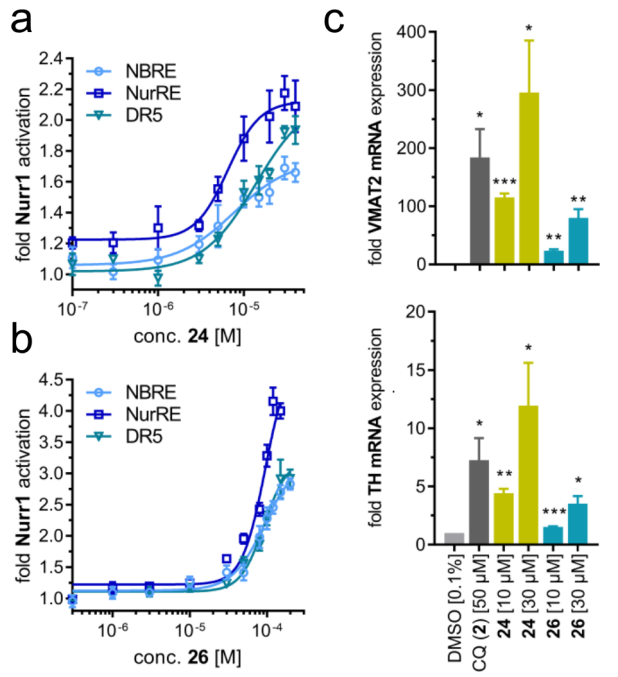

Figure 1. Nurr1 agonism of **24** and **26** in cellular settings. (a, b) Nurr1 agonist activity of (a) **24** and (b) **26** on full-length human Nurr1 as the monomer (NBRE), homodimer (NurRE), and RXR-heterodimer (DR5). Data are the mean ± S.E.M.; n ≥ 3. Individual curves are shown in Figure S4, and corresponding EC_{50} values are listed in Table S1. (c) Effects of **24** and **26** on mRNA expression of vesicular monoamine transporter 2 (VMAT2) and tyrosine hydroxylase (TH) in human astrocytes (T98G). CQ (**2**) for comparison. Nurr1 agonists **24** and **26** strongly promoted Nurr1-regulated VMAT2 and TH expression in a dose-dependent manner. Data are the mean ± S.E.M.; *n* = 4. mRNA levels were determined by qRT-PCR and analyzed by the $2^{-\Delta\Delta Ct}$ method. * p < 0.05, ** p < 0.01, *** p < 0.001 vs. DMSO control (t-test).

Figure S4). Both compounds activated the Nurr1 monomer, homodimer, and RXR-heterodimer on the human Nurr1 response elements NBRE, NurRE, and DR5. In line with the hybrid reporter gene assay data (Figure S5), **24** revealed higher potency compared to **26** and CQ (**2**),[16] while **26** activated the human Nurr1 response elements with higher efficacy. To confirm Nurr1 modulation also in an orthogonal native cellular setting, we determined the effects of **24** and **26** on Nurr1-

https://dx.doi.org/10.1021/acs.jmedchem.0c01779
J. Med. Chem. 2021, 64, 2659−2668

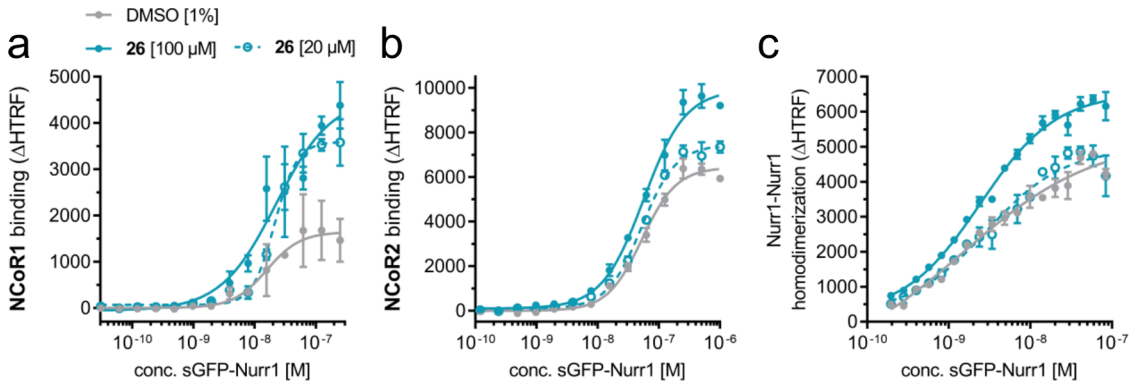

Figure 2. Effects of Nurr1 agonist **26** (20 and 100 μM) on co-regulator recruitment to the Nurr1 LBD in homogeneous time-resolved fluorescence resonance energy transfer (HTRF) assays. (a) Recruitment of Tb^{3+}-cryptate-labeled NCoR1 to the sGFP-labeled Nurr1 LBD. (b) Recruitment of Tb^{3+}-cryptate-labeled NCoR2 to the sGFP-labeled Nurr1 LBD. (c) Homodimerization between the Tb^{3+}-cryptate-labeled and sGFP-labeled Nurr1 LBD. Data are the mean ± SD; $N = 3$. Compound **24** exhibits comparable effects (Figure S6).

regulated gene expression in Nurr1 expressing[17] human astrocytes (T98G) on the mRNA level (Figure 1c). Both **24** and **26** caused a marked induction of vesicular monoamine transporter 2 (VMAT2; SLC18A2) and tyrosine hydroxylase (TH) in a dose-dependent fashion. These results demonstrate Nurr1 activation by **24** and **26** in various cellular settings, and hence, fully characterize the fragments **24** and **26** as Nurr1 agonists useful as lead compounds for medicinal chemistry and as early tools to study Nurr1 biology.

The chloroquinoline **26** comprises a consistent Nurr1 agonist profile in multiple orthogonal cellular settings including hybrid and full-length Nurr1 reporter gene assays and gene expression studies in native cells. In addition, the compound is characterized by reduced nonspecific effects compared to AQ (**1**) and CQ (**2**) and thus seemed suitable as a tool to study regulatory interactions involving in Nurr1 activation in HTRF-based systems. Using inverse Nurr1 agonists, we have previously discovered a ligand-sensitive interaction of Nurr1 with the nuclear receptor co-repressors NCoR1 and NCoR2.[16] However, the previously available Nurr1 agonists AQ (**1**) and CQ (**2**) exhibited very weak (CQ) or no (AQ) effects at all on the binding of these co-regulators to Nurr1.[16] In addition, their nonspecific transcriptional effects put the applicability of AQ (**1**) and CQ (**2**) as tools into question. The regulatory contributions of the bona fide co-repressors NCoR1 and NCoR2 to Nurr1 activation, thus, remained elusive. Initial experiments (not shown) suggested enhanced recruitment of NCoR1 and NCoR2 upon binding of **26** to the Nurr1 LBD, which aligned with our previous finding that these co-regulators are displaced from Nurr1 by inverse agonists. To avoid any photophysical effects of **26** in studying co-regulator recruitment to Nurr1, we determined NCoR1 and NCoR2 binding by titrating the GFP-labeled Nurr1 LBD in the presence of a fixed concentration of **26** and a fixed concentration of the FRET donor-labeled co-regulator peptide. The FRET acceptor concentration was also kept constant throughout the titration by adding respective amounts of free GFP. This setting ensured that any photophysical effects of **26** were constant over the full curve and that an increase in the HTRF signal only resulted from binding of the labeled co-regulator to the labeled Nurr1 LBD. Using this assay setup, we observed a dose-dependent increase in NCoR1 and NCoR2 recruitment to the Nurr1 LBD in the presence of **26** (20 and 100 μM, Figure 2a and 2b) or **24** (100 μM, Figure S6). In line with the previously discovered co-regulator displacement by inverse agonists, these results indicate involvement of NCoR1 and NCoR2 binding in Nurr1 activation. This is further supported by the fact that Nurr1 acts as a constitutive transcriptional activator and markedly recruits NCoR1 and NCoR2 also in the apo state (Figure 2a and 2b, DMSO). In addition to effects on NCoR1 and NCoR2 recruitment, we have previously observed a ligand-sensitive dimerization of the Nurr1 LBD,[16] wherein inverse Nurr1 agonists strongly counteracted Nurr1 homodimer formation. In line with this, the Nurr1 activators **24** and **26** enhanced Nurr1 homodimerization (Figure 2c; Figure S6) as another factor likely involving in Nurr1 activation. This observation aligns with the higher agonist efficacy of **26** on the human Nurr1 homodimer response element NurRE (Figure 1b). Hence, the Nurr1 agonist **26** as a tool in HTRF settings revealed increased recruitment of NCoR1 and NCoR2 to the Nurr1 LBD as well as enhanced Nurr1 homodimerization as contributing factors of Nurr1 activation.

CONCLUSIONS

The available collection of direct Nurr1 modulating small molecules is scarce, limiting further efforts to validate Nurr1 as a drug target. Munoz-Tello et al.[13] have demonstrated that the majority of the putative Nurr1 ligands does not directly interact with the nuclear receptor and thereby characterized the AQ/CQ chemotype as the most suitable starting point for further tool compound development. They have also shown that despite directly activating Nurr1, AQ and CQ have nonspecific effects on transcriptional activity, limiting their applicability as tools to study Nurr1. This aligns with several previously reported activities of the antimalarials[5−13] and with our observation of elevated control gene transcription upon AQ and CQ treatment.

By fragmentation of the AQ/CQ chemotype of Nurr1 activators and systematic SAR elucidation of the fragment-sized chloroquinoline scaffold, we discovered **24** and **26** as novel Nurr1 agonists. Despite providing only moderately increased potency compared to AQ and CQ, these compounds have remarkably lower size and molecular weight, which make them attractive lead compounds for further expansion and optimization by medicinal chemistry. In addition, while **24** also exhibited nonspecific (potentially cytotoxic) effects on transcriptional activity, **26** had no such activity. Thereby, **26** overcomes one limitation of AQ and CQ as Nurr1 ligands, and

https://dx.doi.org/10.1021/acs.jmedchem.0c01779
J. Med. Chem. 2021, 64, 2659−2668

hence, is a valuable early Nurr1 agonist tool to study the receptor's molecular and cellular function. Using **26** for extended functional studies, we confirmed the hypothesis that the inverse Nurr1 agonist responsive[16] co-regulators NCoR1 and NCoR2 are robustly recruited to Nurr1 in the presence of agonists, which together with strengthened Nurr1 homodimerization upon binding of **26** provides insights in the activation mechanism of Nurr1.

EXPERIMENTAL SECTION

Chemistry. *General.* All chemicals and solvents for synthesis were obtained from commercial sources in reagent grade and used without further purification. TLC was performed using TLC plates (silica gel 60 F254, 0.2 mm, Merck or Alugram Xtra Sil G/UV 0.2 mm, Macherey-Nagel) with detection under UV light (254 and 366 nm). Preparative column chromatography was performed using Silicagel 60 (Macherey-Nagel) and solvents of technical grade. Reactions with air- or moisture-sensitive compounds were carried out under an argon atmosphere and in anhydrous solvents. NMR spectra were recorded on Bruker AV 500 and AV 600 spectrometers (Bruker Corporation, Billerica, MA, USA). Chemical shifts (δ) are reported in ppm relative to TMS and coupling constants (J) in Hz. Multiplicity of signals is indicated as s for singlet, d for doublet, t for triplet, q for quartet, and m for multiplet. High-resolution mass spectra were recorded on a MALDI LTQ ORBITRAP XL instrument (Thermo Fisher Scientific) or on a Bruker maXis ESI-Qq-TOF-MS instrument (Bruker). Compound purity was analyzed using a Varian ProStar HPLC (SpectraLab Scientific Inc., Markham, ON, Canada) equipped with a MultoHigh100 Phenyl-5 μ 240 + 4 mm column (CS-Chromatographie Service GmbH, Langerwehe, Germany) using a gradient (H_2O/MeOH 80:20 + 0.1% formic acid isocratic for 5 min to MeOH + 0.1% formic acid after additional 45 min and MeOH + 0.1% formic acid for additional 10 min) at a flow rate of 1 mL/min and UV detection at 245 and 280 nm. All final compounds for biological evaluation had a purity >95% according to the AUC at 245 and 280 nm UV detection. Final compounds from commercial sources were obtained from Sigma Aldrich, Enamine, TCI, Fluorochem, abcr, Apollo Scientific or Life Chemicals and had a purity >95% according to the supplier's certificate.

4-((7-Chloroquinolin-4-yl)amino)phenol (**6**). 4,7-Dichloroquinoline (**12**, 0.99 g, 5.0 mmol, 1.0 equiv), 4-aminophenol (**35**, 0.60 g, 5.5 mmol, 1.1 equiv), and a catalytic amount of potassium iodide were dissolved in ethanol (EtOH, 20 mL), aqueous hydrochloric acid (1.0 mL, 2 N) was added dropwise, and the mixture was stirred under reflux for 14 h. After cooling to room temperature, the crude product was filtered off and washed with EtOH to obtain **6** as a yellow solid in 98% yield. ^{1}H NMR (500 MHz, DMSO-d_6): δ = 10.99 (s, 1H), 9.94 (s, 1H), 8.80 (d, J = 9.1 Hz, 1H), 8.45 (d, J = 7.1 Hz, 1H), 8.14 (d, J = 2.0 Hz, 1H), 7.84 (dd, J = 9.1, 2.1 Hz, 1H), 7.30−7.19 (m, 2H), 7.00−6.93 (m, 2H), 6.62 (d, J = 7.0 Hz, 1H). ^{13}C NMR (126 MHz, DMSO-d_6): δ = 157.09, 155.43, 143.10, 139.02, 138.31, 127.69, 127.23, 127.19 (2C), 125.98, 119.19, 116.49 (2C), 115.66, 99.99. HRMS (MALDI): m/z calculated 271.06327 for $C_{15}H_{12}ClN_2O$, found 271.06403 ([M + H]$^+$).

N^4-(5-Chloronaphthalen-1-yl)-N^1,N^1-diethylpentane-1,4-diamine (**27**). 5-Chloronaphthalen-1-amine (**24**, 89 mg, 0.50 mmol, 1.0 equiv) and 5-(diethylamino)pentan-2-one (**41**, 73 μL, 0.55 mmol, 1.1 equiv) were dissolved in 1,2-dichloroethane (10 mL), molecular sieves (4 Å) were added, and the mixture was stirred at room temperature for 2 h. Then, acetic acid (0.75 mL) was added, and the mixture was stirred at 50 °C for another 2 h. $NaB(OAc)_3H$ (0.32 g, 1.5 mmol, 3.0 equiv) was then added, and the mixture was stirred at 50 °C for 24 h. After quenching with aqueous sodium hydroxide solution (100 mL, 1 M), phases were separated, and the aqueous layer was extracted twice with EtOAc (2x 100 mL). The combined organic layers were dried over Na_2SO_4, and solvents were removed under reduced pressure. The crude product was purified by column chromatography in hexane/EtOAc (10:1) + 2% triethylamine to obtain **27** as a brown oil in 45% yield. ^{1}H NMR (500 MHz, acetone-d_6): δ = 8.14 (dt, J = 8.6, 1.0 Hz, 1H), 7.56 (dd, J = 7.4, 1.0 Hz, 1H), 7.51−7.40 (m, 2H), 7.32 (dd, J = 8.6, 7.3 Hz, 1H), 6.74 (dt, J = 7.3, 1.0 Hz, 1H), 5.43 (s, 1H), 3.80−3.71 (m, 1H), 2.54−2.45 (m, 6H), 1.86−1.78 (m, 1H), 1.69−1.58 (m, 3H), 1.30 (d, J = 6.3 Hz, 3H), 0.98 (t, J = 7.1 Hz, 6H). ^{13}C NMR (126 MHz, acetone-d_6): δ = 144.93, 132.72, 132.44, 129.17, 126.86, 125.65, 124.43, 121.54, 111.98, 105.72, 53.51, 49.24, 47.55 (2C), 35.01, 24.70, 20.63, 12.12 (2C). HRMS (ESI+): m/z calculated 320.1973 for $C_{19}H_{28}ClN_2$, found 320.1982 ([M + H]$^+$).

N^4-(5-Chloronaphthalen-1-yl)-N^1,N^1-dimethylpentane-1,4-diamine (**28**). 5-Chloronaphthalen-1-amine (**24**, 44 mg, 0.25 mmol, 1.0 equiv) and 5-(dimethylamino)pentan-2-one (**42**, 50 mg, 0.33 mmol, 1.3 equiv) were dissolved in 1,2-dichloroethane (10 mL), molecular sieves (4 Å) were added, and the mixture was stirred at room temperature for 2 h. Then, acetic acid (0.75 mL) was added, and the mixture was stirred at 50 °C for another 2 h. $NaB(OAc)_3H$ (0.16 g, 0.75 mmol, 3.0 equiv) was then added, and the mixture was stirred at 50 °C for 24 h. After quenching with aqueous sodium hydroxide solution (50 mL, 1 M), phases were separated, and the aqueous layer was extracted twice with EtOAc (2x 25 mL). The combined organic layers were dried over Na_2SO_4, and solvents were removed under reduced pressure. The crude product was purified by column chromatography with hexane/EtOAc (1:1) and acetone/toluene (20:1) + 2% triethylamine to obtain **28** as a pale brown solid in 25% yield. ^{1}H NMR (500 MHz, acetone-d_6): δ = 8.16 (dt, J = 8.6, 0.9 Hz, 1H), 7.56 (dd, J = 7.4, 1.0 Hz, 1H), 7.51−7.41 (m, 2H), 7.33 (dd, J = 8.6, 7.4 Hz, 1H), 6.73 (dt, J = 7.2, 1.1 Hz, 1H), 3.79−3.73 (m, 1H), 2.50 (t, J = 7.0 Hz, 2H), 2.31 (s, 6H), 1.90−1.61 (m, 4H), 1.30 (d, J = 6.3 Hz, 3H). ^{13}C NMR (126 MHz, acetone-d_6) δ 144.93, 132.71, 132.39, 129.17, 126.88, 125.68, 124.46, 121.67, 111.98, 105.63, 59.56, 49.15, 44.76 (2C), 34.70, 24.32, 20.76. HRMS (ESI+): m/z calculated 291.1628 for $C_{17}H_{24}ClN_2$, found 291.1626 ([M + H]$^+$).

N^4-(8-Chloro-2-methylquinolin-4-yl)-N^1,N^1-diethylpentane-1,4-diamine (**29**). 4,8-Dichloro-2-methylquinoline (**34**, 106 mg, 0.5 mmol, 1.0 equiv) and N^1,N^1-diethylpentane-1,4-diamine (**37**, 0.12 mL, 0.6 mmol, 1.2 equiv) were dissolved in EtOH (6 mL). The mixture was stirred under microwave irradiation at 140 °C for 36 h. After cooling to room temperature, the solvent was removed under vacuum. The crude product was purified by column chromatography using a gradient of hexane/EtOAc (5:1) + 2% triethylamine to hexane/EtOAc (1:1) + 2% triethylamine to obtain **29** as a pale yellow solid in 54% yield. ^{1}H NMR (600 MHz, deuterium oxide): δ = 7.90 (d, J = 8.5 Hz, 1H), 7.75 (d, J = 7.7 Hz, 1H), 7.30 (t, J = 8.0 Hz, 1H), 6.58 (s, 1H), 3.90−3.82 (m, 1H), 3.17 (q, J = 7.2 Hz, 4H), 2.96−2.91 (m, 2H), 2.49 (s, 3H), 1.23 (d, J = 6.3 Hz, 3H), 1.15 (t, J = 7.3 Hz, 6H), 1.06−1.01 (m, 4H). ^{13}C NMR (126 MHz, DMSO-d_6): δ = 160.90, 150.68, 144.75, 131.99, 130.01, 123.74, 121.57, 119.50, 99.90, 52.34, 49.22, 48.27 (2C), 33.93, 25.84, 23.08, 20.47, 11.44 (2C). HRMS (ESI+): m/z calculated 334.2050 for $C_{19}H_{29}ClN_3$, found 334.2055 ([M + H]$^+$).

4-((8-Chloro-2-methylquinolin-4-yl)amino)-2-((diethylamino)-methyl)phenol (**30**). 4,8-Dichloro-2-methylquinoline (**34**, 0.21 g, 1.0 mmol, 1.0 equiv), 4-amino-2-(diethylamino)methyl)phenol dihydrochloride (**36**, 293 mg, 1.1 mmol, 1.1 equiv), and a catalytic amount of potassium iodide were dissolved in EtOH (30 mL), aqueous hydrochloric acid (0.2 mL, 2 N) was added dropwise, and the mixture was stirred under reflux for 20 h. After cooling to room temperature, the mixture was filtered, and the filtrate was concentrated under reduced pressure. The crude product was washed with cold EtOH to obtain **30** as a yellow solid in 51% yield. ^{1}H NMR (500 MHz, deuterium oxide): δ = 8.18 (dd, J = 8.6, 1.2 Hz, 1H), 7.99 (dd, J = 7.7, 1.2 Hz, 1H), 7.60 (t, 1H), 7.46−7.41 (m, 2H), 7.19−7.14 (m, 1H), 6.67 (s, 1H), 4.37 (s, 2H), 3.30 (dq, J = 10.1, 7.2 Hz, 4H), 2.62 (s, 3H), 1.38 (t, J = 7.3 Hz, 6H). ^{13}C NMR (126 MHz, Deuterium Oxide): δ = 156.20, 156.16, 155.95, 135.40, 134.52, 130.28, 129.90, 129.18, 127.36, 124.08, 121.94, 118.78, 117.82, 117.66, 101.72, 52.20, 48.36 (2C), 20.68, 8.83 (2C). HRMS (MALDI): m/z calculated 370.16807 for $C_{21}H_{25}ClN_3O$, found 370.16737 ([M + H]$^+$).

https://dx.doi.org/10.1021/acs.jmedchem.0c01779
J. Med. Chem. 2021, 64, 2659−2668

8-Chloro-*N*-isopropyl-2-methylquinolin-4-amine (**31**). 4,8-Dichloro-2-methylquinoline (**34**, 0.11 g, 0.50 mmol, 1.0 equiv) and propan-2-amine (**38**, 51 μL, 0.60 mmol, 1.2 equiv) were dissolved in EtOH (6.0 mL), and the mixture was stirred for 36 h at 140 °C under microwave irradiation. The solvent was evaporated in vacuum, aqueous sodium hydroxide solution (20 mL) and ethyl acetate (20 mL) were added, phases were separated, and the aqueous layer was extracted two times with ethyl acetate (2x 20 mL). The combined organic layers were dried over Na_2SO_4, and the solvent was evaporated in vacuum. The crude product was purified by column chromatography (hexane/ethyl acetate 5:1 + 2% NEt_3 and hexane/ethyl acetate 1:1 + 2% NEt_3) to obtain the title compound as a yellow oil (15 mg, 13%). ^{1}H NMR (500 MHz, Acetone-d_6): δ = 8.05 (dd, J = 8.5, 1.3 Hz, 1H), 7.70 (dd, J = 7.4, 1.3 Hz, 1H), 7.29−7.22 (m, 1H), 6.54 (s, 1H), 6.14 (d, J = 6.9 Hz, 1H), 4.01−3.90 (m, 1H), 2.54 (s, 3H), 1.34 (d, J = 6.4 Hz, 6H). ^{13}C NMR (126 MHz, acetone-d_6): δ = 160.73, 150.50, 145.82, 133.84, 129.73, 123.57, 120.86, 120.12, 100.33, 44.81, 25.92, 22.31 (2C). HRMS (MALDI): *m/z* calculated 235.09965 for $C_{13}H_{16}ClN_2$, found 235.10002 ($[M + H]^+$).

N-Butyl-8-chloro-2-methylquinolin-4-amine (**32**). 4,8-Dichloro-2-methylquinoline (**34**, 0.11 g, 0.50 mmol, 1.0 equiv) and butan-1-amine (**39**, 73 mg, 1.0 mmol, 2.0 equiv) were dissolved in EtOH (6.0 mL), and the mixture was stirred for 48 h at 140 °C under microwave irradiation. The solvent was evaporated in vacuum, and the crude product was purified by column chromatography (hexane/ethyl acetate 5:1 + 2% NEt_3) to obtain the title compound as a yellow oil (30 mg, 24%). ^{1}H NMR (500 MHz, $CDCl_3$): δ = 7.71−7.64 (m, 2H), 7.20 (t, J = 8.0 Hz, 1H), 6.26 (s, 1H), 3.27−3.22 (m, 2H), 2.62 (s, 3H), 1.72−1.65 (m, 2H), 1.48−1.40 (m, 2H), 0.94 (t, J = 7.4 Hz, 3H). ^{13}C NMR (126 MHz, $CDCl_3$): δ = 159.86, 150.46, 129.63, 123.57, 118.83, 118.61, 99.63, 43.18, 30.92, 25.76, 20.34, 13.85. HRMS (MALDI): *m/z* calculated 249.11530 for $C_{14}H_{18}ClN_2$, found 249.11583 ($[M + H]^+$).

8-Chloro-2-methyl-*N*-(3-methylbutan-2-yl)quinolin-4-amine (**33**). 4,8-Dichloro-2-methylquinoline (**34**, 0.11 g, 0.50 mmol, 1.0 equiv) and 3-methylbutan-2-amine (**40**, 87 mg, 1.0 mmol, 2.0 equiv) were dissolved in EtOH (6.0 mL), and the mixture was stirred for 48 h at 140 °C under microwave irradiation. The solvent was evaporated in vacuum, aqueous sodium hydroxide solution (20 mL) and ethyl acetate (20 mL) were added, phases were separated, and the aqueous layer was extracted two times with ethyl acetate (2x 20 mL). The combined organic layers were dried over Na_2SO_4, and the solvent was evaporated in vacuum. The crude product was purified by column chromatography (hexane/ethyl acetate 5:1 + 2% NEt_3 and hexane/ethyl acetate 1:1 + 2% NEt_3) to obtain the title compound as a green oil (6 mg, 4%). ^{1}H NMR (500 MHz, MeOD): δ = 8.08 (dd, J = 8.5, 1.2 Hz, 1H), 7.70 (dd, J = 7.5, 1.2 Hz, 1H), 7.31−7.26 (m, 1H), 6.49 (s, 1H), 3.57 (quint., J = 6.7 Hz, 1H), 2.53 (s, 3H), 1.95−1.84 (m, J = 6.8, 1H), 1.19 (d, J = 6.6, 3H), 0.94−0.91 (m, 6H). ^{13}C NMR (126 MHz, MeOD): δ = 159.03, 152.19, 130.57, 123.81, 120.37, 118.63, 99.28, 54.29, 32.47, 22.35, 18.62, 17.36, 15.44. HRMS (MALDI): *m/z* calculated 263.13095 for $C_{15}H_{20}ClN_2$, found 263.13157 ($[M + H]^+$).

Hybrid Gal4-Nurr1 Reporter Gene Assay. *Plasmids.* The Gal4-fusion receptor plasmid pFA-CMV-hNURR1-LBD[16] coding for the hinge region and LBD of the canonical isoform of human Nurr1 has been reported previously. The Gal4-VP16[15] fusion protein expressed from plasmid pECE-SV40-Gal4-VP16[22] (Addgene, entry 71728, Watertown, MA, USA) served as a ligand-independent transcriptional inducer for control experiments. pFR-Luc (Stratagene, La Jolla, CA, USA) was used as a reporter plasmid and pRL-SV40 (Promega, Madison, WI, USA) for normalization of transfection efficiency and test compound toxicity. *Assay procedure.* HEK293T cells were grown in DMEM high glucose, supplemented with 10% fetal calf serum (FCS), sodium pyruvate (1 mM), penicillin (100 U/mL), and streptomycin (100 μg/mL) at 37 °C and 5% CO_2. The day before transfection, HEK293T cells were seeded in 96-well plates (3×10^4 cells/well). The medium was changed to Opti-MEM without supplements right before transfection. Transient transfection was performed using the Lipofectamine LTX reagent (Invitrogen, Carlsbad, CA, USA) according to the manufacturer's protocol with pFR-Luc (Stratagene), pRL-SV40 (Promega), and the corresponding Gal4-fusion nuclear receptor plasmid pFA-CMV-hNR-LBD. Five hours after transfection, the medium was changed to Opti-MEM supplemented with penicillin (100 U/mL) and streptomycin (100 μg/mL), now additionally containing 0.1% DMSO and the respective test compound or 0.1% DMSO alone as untreated control. Each concentration was tested in duplicates, and each experiment was performed independently at least three times. The Gal4-VP16 control experiments were carried out in duplicates as well, with at least four independent repeats. Following overnight (12−14 h) incubation with the test compounds, the cells were assayed for luciferase activity using the Dual-Glo™ Luciferase Assay System (Promega) according to the manufacturer's protocol. Luminescence was measured with a Spark 10 M luminometer (Tecan Group AG, Männedorf, Switzerland). Normalization of transfection efficiency and cell growth were done by division of firefly luciferase data by renilla luciferase data and multiplying the value by 1000 resulting in relative light units (RLU). Fold activation was obtained by dividing the mean RLU of a test compound at a respective concentration by the mean RLU of untreated control. The hybrid assay was validated with amodiaquine and chloroquine as reference agonists, which yielded EC_{50} values in agreement with the literature. For dose−response curve fitting and calculation of EC_{50}/IC_{50} values, the equations "[Agonist]/[Inhibitor] vs. response − variable slope (four parameters)" were performed with mean fold activations ± SD using GraphPad Prism (version 7.00, GraphPad Software, La Jolla, CA, USA).

Full-Length Nurr1 Reporter Gene Assays. *Plasmids:* The reporter plasmids pFR-Luc-NBRE,[16] pFR-Luc-NurRE,[16] and pFR-Luc-DR5[16] each containing one copy of the respective human Nurr1 response element NBRE Nl3 (TGATATCGAAAACAAAAGGTCA), NurRE (from POMC; TGATATTTACCTCCAAATGCCA), or DR5 (TGATAGGTTCACCGAAAGGTCA) were described previously. The full length human nuclear receptor Nurr1 (pcDNA3.1-hNurr1-NE; Addgene, entry 102363) and, for DR5, RXRα (pSG5-hRXR[23]) were overexpressed. pFL-SV40 (Promega) was used for normalization of transfection efficacy and evaluation of compound toxicity. *Assay procedure*: HEK293T cells were grown in DMEM high glucose, supplemented with 10% FCS, sodium pyruvate (1 mM), penicillin (100 U/mL), and streptomycin (100 μg/mL) at 37 °C and 5% CO_2. The day before transfection, HEK293T cells were seeded in 96-well plates (3×10^4 cells/well). The medium was changed to Opti-MEM without supplements right before transfection. Transient transfection was performed using the Lipofectamine LTX reagent (Invitrogen) according to the manufacturer's protocol with pFR-Luc-NBRE,[16] pFR-Luc-NurRE[16] or pFR-Luc-DR5,[16] pRL-SV40 (Promega), the human full length receptor plasmid pcDNA3.1-hNurr1-NE, and, for DR5, also pSG5-hRXR.[23] Five hours after transfection, the medium was changed to Opti-MEM supplemented with penicillin (100 U/mL) and streptomycin (100 μg/mL), now additionally containing 0.1% DMSO and the respective test compound or 0.1% DMSO alone as untreated control. For full dose−response characterization, each concentration was tested in duplicates and each experiment was performed independently at least three times. Following overnight (12−14 h) incubation with the test compounds, the cells were assayed for luciferase activity using a Dual-Glo™ Luciferase Assay System (Promega) according to the manufacturer's protocol. Luminescence was measured with a Spark 10 M luminometer (Tecan Group AG). Normalization of transfection efficiency and cell growth were done by division of firefly luciferase data by renilla luciferase data and multiplying the value by 1000 resulting in RLU. Fold activation was obtained by dividing the mean RLU of a test compound at a respective concentration by the mean RLU of untreated control. The full length Nurr1 reporter gene assays were validated with amodiaquine and chloroquine as reference agonists.

Nurr1 Co-Regulator Recruitment Assays. Interaction of co-regulator peptides to the Nurr1-LBD was studied in a homogeneous time-resolved fluorescence resonance energy transfer (HT-FRET) assay system. Terbium cryptate as streptavidin conjugate (Tb-SA; Cisbio Bioassays, Codolet, France) was used as FRET donor for stable coupling to biotinylated co-regulator peptides NCoR1 or

https://dx.doi.org/10.1021/acs.jmedchem.0c01779
J. Med. Chem. 2021, 64, 2659−2668

NCoR2. As FRET acceptor, recombinant Nurr1-LBD protein[16] fused to sGFP was used, which has been reported previously. GFP-Nurr1-LBD was titrated against biotinylated NCoR1 (1 nM) or NCoR2 (18 nM) copeptide and Tb-SA (2 or 12 nM, respectively) in the presence of a fixed concentration (20 or 100 μM, in assay buffer containing 1% DMSO) of the respective ligand or 1% DMSO. To maintain a constant GFP concentration, free GFP protein was added to the dilution series. The experiments were performed in HTRF assay buffer (150 mM KF, 25 mM HEPES pH 7.5 (KOH), 5% (w/v) Glycerol, supplemented with 0.1% (w/v) CHAPS and 5 mM DTT) with 1% DMSO in an assay volume of 20 μL. All HTRF experiments were carried out in a 384-well format using white flat bottom polystyrol microtiter plates (Greiner Bio-One, Frickenhausen, Germany), and each concentration was tested in technical triplicates. After 1 h incubation at room temperature, fluorescence intensities after excitation at 340 nm were recorded at 520 nm for GFP acceptor fluorescence and 620 nm for Tb-SA donor fluorescence on a SPARK plate reader (Tecan Group Ltd.). FI520nm was divided by FI620nm and multiplied with 10,000 to give a dimensionless HTRF signal. ΔHTRFs were calculated as differences between each individual HTFR value and the corresponding untreated control (1% DMSO) of the same dissolution series. For the dose−response curve fitting, the equation "[Agonist] vs. response − variable slope (four parameters)" was performed with three replicate values of ΔHTRF using GraphPad Prism (version 7.00, GraphPad Software). The co-regulator peptides were purchased from Eurogentec (Seraing, Belgium), and sequences were the following: nuclear receptor co-repressor 1 (NCoR1) nuclear receptor-interaction domain 1 (ID1), Biotin-GMGQVPRTHRLI-TLADHICQIITQDFARN-COOH; and NCoR2 ID2, Biotin-SQAV-QEHASTNMGLEAIIRKALMGKYDQW-COOH.

Nurr1 Homodimerization Assay. Modulation of Nurr1 LBD homodimerization was studied in an HT-FRET assay setup using the biotinylated recombinant Nurr1 LBD[16] and GFP-Nurr1 LBD. Assay solutions were prepared in HTRF assay buffer supplemented with 0.1% (w/v) CHAPS and 5 mM DTT as well as 1% DMSO with test compounds **24** (100 μM) and **26** (20 or 100 μM) or DMSO alone as negative control. The biotinylated Nurr1 LBD (0.375 nM) and Tb-SA (0.75 nM) served as the FRET donor complex, which was kept constant, while the GFP-coupled protein as the FRET acceptor was varied in concentration. Titration of the GFP-Nurr1 LBD started at 500 nM, and each concentration was tested in technical triplicates. Accordingly, free GFP was added to keep the total GFP content stable throughout the entire series in order to suppress artifacts from changes in the degree of diffusion-enhanced FRET. The samples were equilibrated at room temperature for 2 h before FI520nm and FI620nm were recorded after excitation at 340 nm, and the HTRF signal, ΔHTRF, and dose−response curves were calculated as described above.

Quantification of Nurr1-Regulated mRNA Expression in T98G Cells by qRT-PCR. T98G cells were grown in 6-well plates (2.5×10^5 cells/well) in DMEM high glucose, supplemented with 10% FCS, sodium pyruvate (1 mM), penicillin (100 U/mL), and streptomycin (100 μg/mL) at 37 °C and 5% CO_2. Before incubation with test compounds, the medium was changed to DMEM supplemented with 1% charcoal-stripped FCS, sodium pyruvate (1 mM), penicillin (100 U/mL), and streptomycin (100 μg/mL) for 24 h. For gene expression analysis, the cells were incubated with **2** (50 μM), **24** (10 or 30 μM), **26** (10 or 30 μM), or 0.1% DMSO as untreated control for 8 h. The cells were then harvested and directly used for RNA extraction. Total RNA (3 μg) was extracted from T98G cells by the E.Z.N.A. Total RNA Kit I (R6834−02, Omega Bio-Tek, Inc., Norcross, GA). RNA was reverse-transcribed into cDNA using the High-Capacity RNA-to-cDNA Kit (4387406, Thermo Fischer Scientific, Inc.) according to the manufacturer's protocol. Nurr1 target gene expression was evaluated by qRT-PCR analysis with a StepOnePlus System (Life Technologies, Carlsbad, CA) using Power SYBR Green (Life Technologies; 12.5 μL/well). Each sample was set up in duplicates and repeated in four independent experiments. The expression was quantified by the comparative $2^{-\Delta\Delta Ct}$ method, and glyceraldehyde 3-phosphate dehydrogenase (GAPDH) served as the reference gene. Primer sequences for Nurr1 target genes vesicular monoamine transporter 2 (VMAT2) and tyrosine hydroxylase (TH) were obtained from OriGene (OriGene Technologies Inc., Rockville, MD, USA). The following PCR primers were used: hGAPDH: 5′-ATA TGA TTC CAC CCA TGG CA (fw), 5′-GAT GAT GAC CCT TTT GGC TC (rev), hVMAT2: 5′-GCT ATG CCT TCC TGC TGA TTG C (fw), 5′-CCA AGG CGA TTC CCA TGA CGT T (rev), and hTH: 5′-GCT GGA CAA GTG TCA TCA CCT G (fw), and 5′-CCT GTA CTG GAA GGC GAT CTC A (rev).

■ ASSOCIATED CONTENT

Supporting Information

The Supporting Information is available free of charge at https://pubs.acs.org/doi/10.1021/acs.jmedchem.0c01779.

Control experiments; nonspecific effects and cytotoxicity; raw luminescence data; effects of Nurr1 agonist 24; summarized cellular Nurr1 modulatory activities; and WST-1 toxicity assay (PDF)

HPLC traces of compounds synthesized in this study (PDF)

Molecular formula strings with structures and activity data (csv)

■ AUTHOR INFORMATION

Corresponding Author

Daniel Merk − *Institute of Pharmaceutical Chemistry, Goethe University, D-60438 Frankfurt, Germany;* orcid.org/0000-0002-5359-8128; Email: merk@pharmchem.uni-frankfurt.de

Authors

Sabine Willems − *Institute of Pharmaceutical Chemistry, Goethe University, D-60438 Frankfurt, Germany*

Julia Ohrndorf − *Institute of Pharmaceutical Chemistry, Goethe University, D-60438 Frankfurt, Germany*

Whitney Kilu − *Institute of Pharmaceutical Chemistry, Goethe University, D-60438 Frankfurt, Germany*

Jan Heering − *Fraunhofer Institute for Translational Medicine and Pharmacology ITMP, D-60596 Frankfurt am Main, Germany*

Complete contact information is available at: https://pubs.acs.org/10.1021/acs.jmedchem.0c01779

Author Contributions

All authors have given approval to the final version of the manuscript.

Notes

The authors declare no competing financial interest.

■ ACKNOWLEDGMENTS

This research was financially supported by the Aventis Foundation (Life Science Bridge Award to D.M.) and the LOEWE center Translational Medicine and Pharmacology (TMP). Gal4-VP16 was a gift from Lea Sistonen (Addgene plasmid # 71728 ; http://n2t.net/addgene:71728 ; RRID:Addgene_71728). pcDNA3.1-hNurr1-NE was a gift from Shu Leong Ho (Addgene plasmid # 102363 ; http://n2t.net/addgene:102363 ; RRID:Addgene_102363).

■ ABBREVIATIONS

AQ, amodiaquine; CQ, chloroquine; DR5, direct repeats spaced by five nucleotides; FRET, fluorescence resonance

energy transfer; GFP, green fluorescent protein; HTRF, homogeneous time-resolved fluorescence resonance energy transfer; LBD, ligand binding domain; LE, ligand efficiency; LLE, lipophilic ligand efficiency; NBRE, NGFI-B response element; NCoR1, nuclear receptor co-repressor 1; NCoR2, nuclear receptor co-repressor 2; Nurr1, nuclear receptor related 1; NurRE, Nur-response element; PD, Parkinson's Disease; qRT-PCR, quantitative real-time polymerase chain reaction; SAR, structure−activity relationship; SILE, size-independent ligand efficiency; TH, tyrosine hydroxylase; VMAT2, vesicular monoamine transporter 2; VP16, Herpes simplex virus protein vmw65

REFERENCES

(1) Wang, Z.; Benoit, G.; Liu, J.; Prasad, S.; Aarnisalo, P.; Liu, X.; Xu, H.; Walker, N. P.; Perlmann, T. Structure and Function of Nurr 1 Identifies a Class of Ligand-Independent Nuclear Receptors. *Nature* **2003**, *423*, 555−560.

(2) Decressac, M.; Volakakis, N.; Björklund, A.; Perlmann, T. NURR1 in Parkinson Disease—From Pathogenesis to Therapeutic Potential. *Nat. Rev. Neurol.* **2013**, *9*, 629−636.

(3) Kim, C.-H.; Han, B.-S.; Moon, J.; Kim, D.-J.; Shin, J.; Rajan, S.; Nguyen, Q. T.; Sohn, M.; Kim, W.-G.; Han, M.; Jeong, I.; Kim, K.-S.; Lee, E.-H.; Tu, Y.; Naffin-Olivos, J. L.; Park, C.-H.; Ringe, D.; Yoon, H. S.; Petsko, G. A.; Kim, K.-S. Nuclear Receptor Nurr1 Agonists Enhance Its Dual Functions and Improve Behavioral Deficits in an Animal Model of Parkinson's Disease. *Proc. Natl. Acad. Sci.* **2015**, *112*, 8756−8761.

(4) Rajan, S.; Jang, Y.; Kim, C. H.; Kim, W.; Toh, H. T.; Jeon, J.; Song, B.; Serra, A.; Lescar, J.; Yoo, J. Y.; Beldar, S.; Ye, H.; Kang, C.; Liu, X. W.; Feitosa, M.; Kim, Y.; Hwang, D.; Goh, G.; Lim, K. L.; Park, H. M.; Lee, C. H.; Oh, S. F.; Petsko, G. A.; Yoon, H. S.; Kim, K.-S. PGE1 and PGA1 Bind to Nurr1 and Activate Its Transcriptional Function. *Nat. Chem. Biol.* **2020**, *16*, 876−886.

(5) De Bruyn, T.; Van Westen, G. J. P.; IJzerman, A. P.; Stieger, B.; De Witte, P.; Augustijns, P. F.; Annaert, P. P. Structure-Based Identification of Oatp1b1/3 Inhibitors. *Mol. Pharmacol.* **2013**, *83*, 1257−1267.

(6) Lee, S. G.; Alpert, T. D.; Jez, J. M. Crystal Structure of Phosphoethanolamine Methyltransferase from Plasmodium Falciparum in Complex with Amodiaquine. *Bioorganic Med. Chem. Lett.* **2012**, *22*, 4990−4993.

(7) Ren, S.; Zeng, J.; Mei, Y.; Zhang, J. Z. H.; Yan, S. F.; Fei, J.; Chen, L. Discovery and Characterization of Novel, Potent, and Selective Cytochrome P450 2J2 Inhibitors. *Drug Metab. Dispos.* **2012**, *41*, 60−71.

(8) O'Neill, P. M.; Park, B. K.; Shone, A. E.; Maggs, J. L.; Roberts, P.; Stocks, P. A.; Biagini, G. A.; Bray, P. G.; Gibbons, P.; Berry, N.; Winstanley, P. A.; Mukhtar, A.; Bonar-Law, R.; Hindley, S.; Bambal, R. B.; Davis, C. B.; Bates, M.; Hart, T. K.; Gresham, S. L.; Lawrence, R. M.; Brigandi, R. A.; Gomez-delas-Heras, F. M.; Gargallo, D. V.; Ward, S. A. Candidate Selection and Preclinical Evaluation of N-Tert-Butyl Isoquine (GSK369796), an Affordable and Effective 4-Aminoquinoline Antimalarial for the 21st Century. *J. Med. Chem.* **2009**, *52*, 1408−1415.

(9) Kim, T. H.; Kim, H. K.; Hwang, E. S. Novel Anti-adipogenic Activity of Anti-malarial Amodiaquine Through Suppression of PPARγ Activity. *Arch. Pharmacal Res.* **2017**, *40*, 1336−1343.

(10) Tang, Y.; Wu, Q.; Beland, F. A.; Chen, S.; Fang, J. L. Apoptosis Contributes to the Cytotoxicity Induced by Amodiaquine and Its Major Metabolite N-Desethylamodiaquine in Hepatic Cells. *Toxicol. Vitr.* **2020**, *62*, No. 104669.

(11) Gordon, D. E.; Jang, G. M.; Bouhaddou, M.; Xu, J.; Obernier, K.; White, K. M.; O'Meara, M. J.; Rezelj, V. V.; Guo, J. Z.; Swaney, D. L.; Tummino, T. A.; Hüttenhain, R.; Kaake, R. M.; Richards, A. L.; Tutuncuoglu, B.; Foussard, H.; Batra, J.; Haas, K.; Modak, M.; Kim, M.; Haas, P.; Polacco, B. J.; Braberg, H.; Fabius, J. M.; Eckhardt, M.; Soucheray, M.; Bennett, M. J.; Cakir, M.; McGregor, M. J.; Li, Q.; Meyer, B.; Roesch, F.; Vallet, T.; Mac Kain, A.; Miorin, L.; Moreno, E.; Naing, Z. Z. C.; Zhou, Y.; Peng, S.; Shi, Y.; Zhang, Z.; Shen, W.; Kirby, I. T.; Melnyk, J. E.; Chorba, J. S.; Lou, K.; Dai, S. A.; Barrio-Hernandez, I.; Memon, D.; Hernandez-Armenta, C.; Lyu, J.; Mathy, C. J. P.; Perica, T.; Pilla, K. B.; Ganesan, S. J.; Saltzberg, D. J.; Rakesh, R.; Liu, X.; Rosenthal, S. B.; Calviello, L.; Venkataramanan, S.; Liboy-Lugo, J.; Lin, Y.; Huang, X. P.; Liu, Y.; Wankowicz, S. A.; Bohn, M.; Safari, M.; Ugur, F. S.; Koh, C.; Savar, N. S.; Tran, Q. D.; Shengjuler, D.; Fletcher, S. J.; O'Neal, M. C.; Cai, Y.; Chang, J. C. J.; Broadhurst, D. J.; Klippsten, S.; Sharp, P. P.; Wenzell, N. A.; Kuzuoglu-Ozturk, D.; Wang, H. Y.; Trenker, R.; Young, J. M.; Cavero, D. A.; Hiatt, J.; Roth, T. L.; Rathore, U.; Subramanian, A.; Noack, J.; Hubert, M.; Stroud, R. M.; Frankel, A. D.; Rosenberg, O. S.; Verba, K. A.; Agard, D. A.; Ott, M.; Emerman, M.; Jura, N.; von Zastrow, M.; Verdin, E.; Ashworth, A.; Schwartz, O.; d'Enfert, C.; Mukherjee, S.; Jacobson, M.; Malik, H. S.; Fujimori, D. G.; Ideker, T.; Craik, C. S.; Floor, S. N.; Fraser, J. S.; Gross, J. D.; Sali, A.; Roth, B. L.; Ruggero, D.; Taunton, J.; Kortemme, T.; Beltrao, P.; Vignuzzi, M.; García-Sastre, A.; Shokat, K. M.; Shoichet, B. K.; Krogan, N. J. A SARS-CoV-2 Protein Interaction Map Reveals Targets for Drug Repurposing. *Nature* **2020**, *583*, 459−468.

(12) Nolan, K. A.; Caraher, M. C.; Humphries, M. P.; Bettley, H. A. A.; Bryce, R. A.; Stratford, I. J. In Silico Identification and Biochemical Evaluation of Novel Inhibitors of NRH:Quinone Oxidoreductase 2 (NQO2). *Bioorganic Med. Chem. Lett.* **2010**, *20*, 7331−7336.

(13) Munoz-Tello, P.; Lin, H.; Khan, P.; De Vera, I. M. S.; Kamenecka, T. M.; Kojetin, D. J. Assessment of NR4A Ligands That Directly Bind and Modulate the Orphan Nuclear Receptor Nurr1. *J. Med. Chem.* **2020**, *63*, 15639−15654.

(14) Apelt, J.; Ligneau, X.; Pertz, H. H.; Arrang, J.; Ganellin, C. R.; Schwartz, J.-C.; Schunack, W.; Stark, H. Development of a New Class of Nonimidazole Histamine H 3 Receptor Ligands with Combined Inhibitory Histamine N-Methyltransferase Activity. *J. Med. Chem.* **2002**, *45*, 1128−1141.

(15) Sadowski, I.; Ma, J.; Triezenberg, S.; Ptashne, M. GAL4-VP16 Is an Unusually Potent Transcriptional Activator. *Nature* **1988**, *335*, 563−564.

(16) Willems, S.; Kilu, W.; Ni, X.; Chaikuad, A.; Knapp, S.; Heering, J.; Merk, D. The Orphan Nuclear Receptor Nurr1 Is Responsive to Non-steroidal Anti-inflammatory Drugs. *Commun. Chem.* **2020**, *3*, 85.

(17) Karki, K.; Li, X.; Jin, U. H.; Mohankumar, K.; Zarei, M.; Michelhaugh, S. K.; Mittal, S.; Tjalkens, R.; Safe, S. Nuclear Receptor 4A2 (NR4A2) Is a Druggable Target for Glioblastomas. *J. Neurooncol.* **2020**, *146*, 25−39.

(18) Hopkins, A. L.; Keserü, G. M.; Leeson, P. D.; Rees, D. C.; Reynolds, C. H. The Role of Ligand Efficiency Metrics in Drug Discovery. *Nat. Rev. Drug Discov.* **2014**, *13*, 105−121.

(19) Tetko, I. V.; Tanchuk, V. Y. Application of Associative Neural Networks for Prediction of Lipophilicity in ALOGPS 2.1 Program. *J. Chem. Inf. Comput. Sci.* **2002**, *42*, 1136−1145.

(20) Niu, Y. R.; Wei, B.; Chen, B.; Xu, L. H.; Jing, X.; Peng, C. L.; Ma, T. Z. Amodiaquine-Induced Reproductive Toxicity in Adult Male Rats. *Mol. Reprod. Dev.* **2016**, *83*, 174−182.

(21) Bernuau, J.; Larrey, D.; Campillo, B.; Degott, C.; Verdier, F.; Rueff, B.; Pessayre, D.; Benhamou, J. P. Amodiaquine-Induced Fulminant Hepatitis. *J. Hepatol.* **1988**, *6*, 109−112.

(22) Budzyński, M. A.; Puustinen, M. C.; Joutsen, J.; Sistonen, L. Uncoupling Stress-Inducible Phosphorylation of Heat Shock Factor 1 from Its Activation. *Mol. Cell. Biol.* **2015**, *35*, 2530−2540.

(23) Merk, D.; Lamers, C.; Ahmad, K.; Carrasco Gomez, R.; Schneider, G.; Steinhilber, D.; Schubert-Zsilavecz, M. Extending the Structure-Activity Relationship of Anthranilic Acid Derivatives as Farnesoid x Receptor Modulators: Development of a Highly Potent Partial Farnesoid X Receptor Agonist. *J. Med. Chem.* **2014**, *57*, 8035−8055.

https://dx.doi.org/10.1021/acs.jmedchem.0c01779
J. Med. Chem. 2021, 64, 2659−2668